4 Photon flux, brilliance, peak brilliance

When characterising synchrotron radiation sources, it is common practice to specify the spectrum of the photon flux or brilliance instead of the spectrum of the synchrotron radiation beam power. The conversion of the power spectrum into a flux spectra is done by an ad hoc quantisation of the result obtained in the classical way. This is justified by the fact that the accelerated particles are obviously in states with high quantum numbers, i.e. (from the point of view of quantum mechanics) at the classical limit.

Transition to photon flux spectrum through quantisation

$$W_\gamma = \hbar\omega. \tag{4.1}$$

This can be used to specify the

$$\begin{aligned} \text{spectral photon flux} &:= \frac{\text{number of photons}}{\text{time, relative band width}} \\ \frac{\mathrm{d}\dot{n}}{\mathrm{d}W_\gamma/W_\gamma} &= \frac{\mathrm{d}\dot{n}}{\mathrm{d}\omega/\omega} = \frac{1}{\hbar}\frac{\mathrm{d}P}{\mathrm{d}\omega} \\ &= \frac{P_\mathrm{S}}{W_{\gamma c}}\left(S_{\mathrm{S}\sigma}(W_\gamma) + S_{\mathrm{S}\pi}(W_\gamma)\right) \end{aligned} \tag{4.2}$$

$$\left[\frac{\mathrm{d}\dot{n}}{\mathrm{d}W_\gamma/W_\gamma}\right] = \frac{\mathrm{s}^{-1}}{0.1\%\mathrm{bw}} \tag{4.3}$$

with the critical energy

$$W_{\gamma c} := \hbar\omega_c. \tag{4.4}$$

This can be applied accordingly to the spectral and angular distribution and the parameters related to the stored ring current. If the angular distribution is integrated over a limited solid angle range (or a limited area at a fixed distance), the result is the flux through a pinhole, a quantity often used to characterise the source.

The most commonly used quantity to characterise the performance of synchrotron radiation sources is the (time-averaged) *brilliance* (also *brightness*) (see e.g. Shen 2001):

$$\begin{aligned} \text{brilliance} &= \frac{\text{spectral flux}}{\text{source size} \times \text{divergence}} \\ B &:= \frac{\mathrm{d}\dot{n}}{\mathrm{d}W_\gamma/W_\gamma \sigma_x \sqrt{\sigma_{x'}^2 + \sigma_{\gamma'}^2}\sigma_y\sqrt{\sigma_{y'}^2 + \sigma_{\gamma'}^2}} \end{aligned} \tag{4.5}$$

The brilliance thus additionally refers to properties of the electron beam, or more precisely, its phase space volume. The smaller this phase space volume, the greater the brilliance.

Remark. The source divergence is composed of the divergence of the electron beam $\sigma_{x'}$ and $\sigma_{y'}$ and the divergence of the photon beam $\sigma_{\gamma'}$. If the emission averaged over a longitudinal path (as in the case of the undulator), then instead of the size of the electron beam cross-section the apparent source size is considered, which additionally takes into account the electron beam divergence over the length of the undulator.

Remark. The definition of brilliance given here is a rather heuristic one. A fundamental definition can be given in the context of Gaussian optics; the interested reader is referred to Kwang-Je Kim 1986 and Huang 2013, for example.

The brilliance is directly related to the transverse coherence of the radiation.

For the coherent flow, we obtain

$$\frac{\mathrm{d}\dot{n}_c}{\mathrm{d}W_\gamma/W_\gamma} = \left(\frac{\lambda}{2}\right)^2 B \tag{4.6}$$

and for the coherent fraction

$$p_c = \frac{\mathrm{d}\dot{n}_c/\mathrm{d}W_\gamma/W_\gamma}{\mathrm{d}\dot{n}/\mathrm{d}W_\gamma/W_\gamma} = \frac{\lambda^2}{4\sigma_x\sqrt{\sigma_{x'}^2+\sigma_{\gamma'}^2}\,\sigma_y\sqrt{\sigma_{y'}+\sigma_{\gamma'}^2}} \tag{4.7}$$

This contribution is also $< 1\%$ for 3rd-generation sources. These relationships can also be rigorously demonstrated within the framework of Gaussian optics (Kwang-Je Kim 1986; Kwang-Je Kim 1989; Huang 2013).

Flux and brilliance – examples

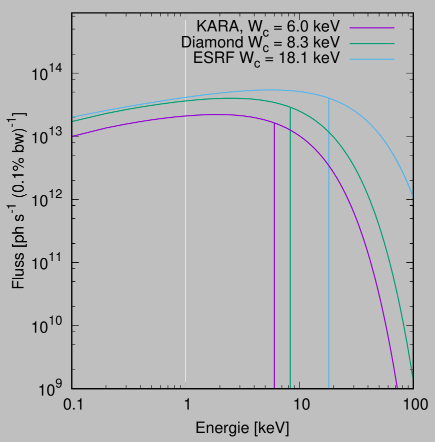

Figure 21: Integral photon flux at the bending magnet: KARA, Diamond and ESRF

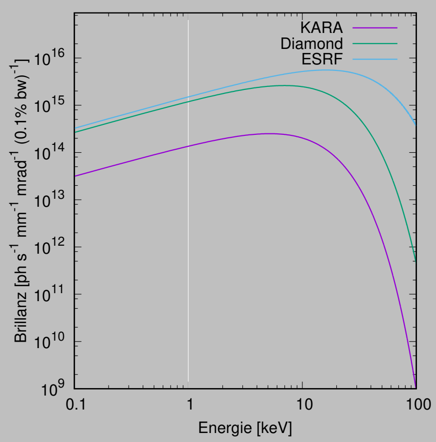

Figure 22: Brilliance at the bending magnet: KARA, Diamond and ESRF

Finally, to also take the radiation pulse length into account, one can consider not only the transverse but also the longitudinal phase space volume of the electron beam. The brilliance per radiation pulse related to the pulse duration is called peak brilliance (*peak brilliance*).

$$\hat{B} := \frac{B}{\sigma_\tau \nu} \tag{4.8}$$

with σ_τ: pulse duration, ν repetition frequency. This quantity particularly highlights the special source properties of free-electron lasers, which are characterised by an extremely high photon number in the single pulse (due to the coherent emission of all electrons in the electron bunch) and an extremely short pulse duration (<100 fs).

At this point, a critical note is in order.

Dedicated synchrotron radiation sources

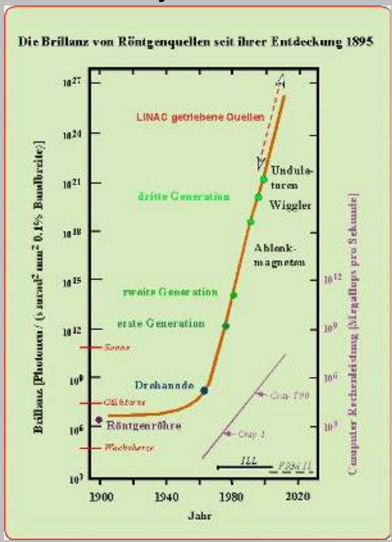

“Moore’s Law” for synchrotron radiation sources

The increase in the performance of synchrotron radiation sources over the last 30 years is most dramatically expressed in the brilliance. This increase in brilliance is due to three developments:

- The construction of large synchrotron radiation sources with energies in the range 6..8 GeV (ESRF, APS, SpRing8, PETRAIII) with a corresponding increase in radiation power (but: too much radiation is not good either; the enormous radiation power at SpRing8 (8 GeV) causes considerable heat load and radiation protection problems)
- The installation of *insertion devices*
- The reduction of the electron beam emittance

In the last case, the increase in brilliance is not accompanied by an increase in flux.

Show me your brilliance plot, ...

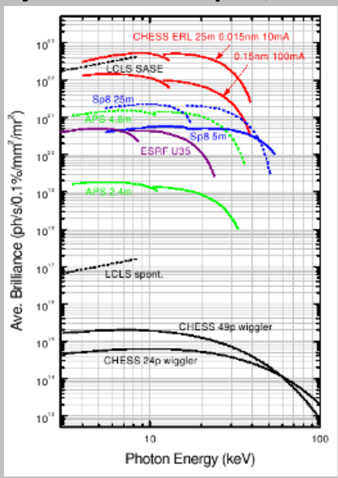

Figure 23: Brilliance of the Cornell ERL

... and I'll tell you who you are

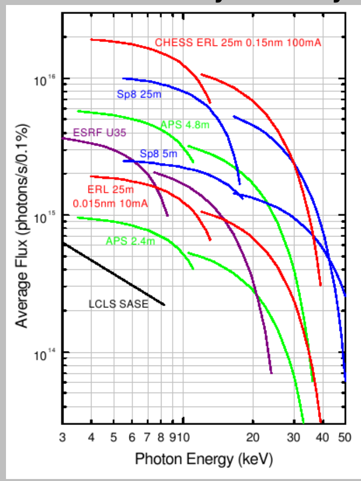

Figure 24: Flux of the Cornell-ERL

Now, the development of 4th generation synchrotron radiation sources is also bringing further increases in brilliance, although these do not necessarily go hand in hand with a corresponding further increase in the photon flux. This raised the question of what the user ultimately needs: Flux, brilliance or even peak brilliance?

The answer is: what the user ultimately needs is as many photons as possible in his detector. Depending on the experiment, however, the requirements on the source properties (high brilliance, high peak brilliance or high integral photon flux) can be quite different.

References

Hofmann, Albert (2004). *The Physics of Synchrotron Radiation*. Cambridge Monographs on Particle Physics, Nuclear Physics and Cosmology. Cambridge: Cambridge University Press. ISBN: 978-0-521-30826-7. DOI: 10.1017/CBO9780511534973.

Huang, Z (2013). "Brightness and Coherence of Synchrotron Radiation and FELs". In: *Proceedings of IPAC 2013*. IPAC 2013. Shanghai, China, p. 5. URL: accelconf.web.cern.ch/AccelConf/IPAC2013/papers/moycb101.pdf.

Kim, Kwang-Je (May 1986). "Brightness, Coherence and Propagation Characteristics of Synchrotron Radiation". In: *Nuclear Instruments and Methods in Physics Research Section A: Accelerators, Spectrometers, Detectors and Associated Equipment* 246.1-3, pp. 71–76. ISSN: 01689002. DOI: 10.1016/0168-9002(86)90048-3.

Kim, Kwang-Je (Apr. 1, 1989). "Characteristics of Synchrotron Radiation". In: *AIP Conference Proceedings* 184.1, pp. 565–632. ISSN: 0094-243X. DOI: 10.1063/1.38046.

Shen, Qun (2001). *X-Ray Flux, Brilliance and Coherence of the Proposed Cornell Energy-recovery Synchrotron Source*. CHESS Technical Memo 01-002. Cornell University, Ithaca, NY, p. 18. URL: https://www.classe.cornell.edu/rsrc/Home/Research/ERL/ErlPubs2001/ERLPub01_4.pdf.

5 Undulators and Wigglers — Introduction

Modern synchrotron radiation sources (so-called 3rd generation sources) are characterised by the fact that they are optimised for operation with special magnet structures to generate particularly intense synchrotron radiation. These magnet structures are installed in magnet-free straight sections (*insertions*) and are therefore referred to generically as *insertion devices*.

Insertion devices play a role not only as local radiation sources in 3rd generation storage ring sources, they are also used to damp the transversal electron motion (the so-called betatron oscillations) and are an essential component of free-electron lasers. In the latter context in particular, we will come back to the physics of undulators again later.

The planar undulator/wiggler

Idea:
Multiple deflection and intensity or amplitude multiplication

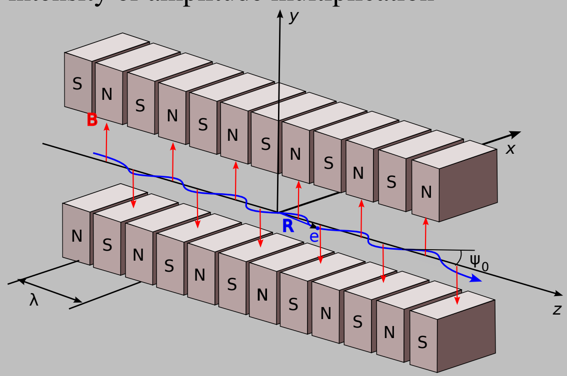

Figure 25: Schematic of an insertion device: alternating magnetic field and sinusoidal path.

Common feature of insertion devices: magnetic structure consisting of several dipoles with zero total deflection and zero total offset.

Most important example: planar harmonic magnetic field:

$$B(z) = B_y = B_0 \cos\left(\frac{2\pi}{\lambda_\mathrm{u}} z\right) = B_0 \cos k_\mathrm{u} z \tag{5.1}$$

with λ_u : period length of the insertion device.

If the field B_0 is relatively weak, the following applies to the motion of ultrarelativistic particles along the z-axis in a good approximation

$$x(z) = a \cos k_\mathrm{u} z, \quad \frac{\mathrm{d}x}{\mathrm{d}z} = -a k_\mathrm{u} \sin k_\mathrm{u} z = -\psi_0 \sin k_\mathrm{u} z \tag{5.2}$$

with

$$\begin{aligned} a &:= \text{amplitude of the trajectory} \\ \psi_0 &:= \text{maximum angle of the trajectory against the } z\text{-axis} \end{aligned} \tag{5.3}$$

The maximum angle of the trajectory, in relation to the ‘aperture angle of the emitted radiation, is an important parameter for classifying the insertion devices; it plays a crucial role in determining the properties of the emitted radiation.

Undulator parameter:

$$K_\mathrm{u} :\approx \frac{\psi_0}{1/\gamma} \tag{5.4}$$

This equation reflects the essential meaning of the undulator parameter, but it is not a completely correct definition. We will give the exact definition later.

With regard to K_u, insertion devices can be divided into two main classes:

- *Wiggler*: $K_\mathrm{u} \gg 1$
  - strongly modulated field
  - essentially incoherent addition of the fields radiated at each pole ($P_\mathrm{W} \propto N_\mathrm{p}$ with N_p =number of poles)
- *Undulator*: $K_\mathrm{u} \lesssim 1$
  - weakly modulated field
  - ‘Overlap of the radiation cones of
  - partially coherent ’undulator radiation, constructive interference for certain wavelengths
  - quasimonochromatic radiation with $P_\mathrm{u} \propto N_\mathrm{u}^2$, N_u =number of periods

Photon flux of insertion devices

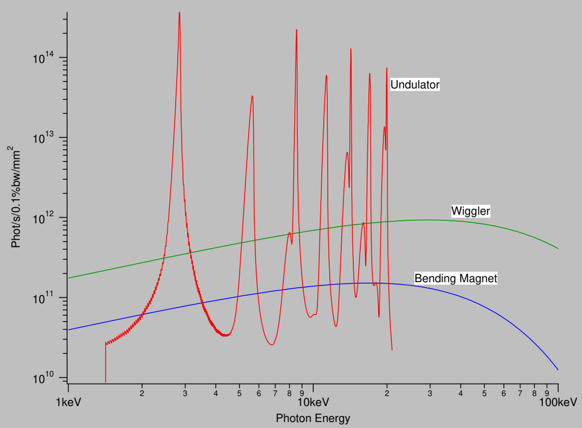

Figure 26: Spectral photon flux (calculated) of a bending magnet, a 1.8 T wiggler and the U35 undulator at the European Synchrotron Radiation Facility (ESRF)

Remark. As we shall see later, the motion of the electron in the undulator field is in reality not a pure sinusoidal oscillation but a periodic motion with Fourier components of higher order as well. This means that the radiation spectrum not only shows the fundamental frequency (in the example of Fig. 26 at about 2.7 keV), but also higher harmonics at integer multiples of this fundamental frequency.

The wiggler case seems to be the more intuitive one at first. N-fold deflection leads to an N-fold increase in the radiated intensity while preserving the spectral properties of the radiation.

In fact, the physical description for the undulator case, especially in the limit of very weak deflection, is the simpler one. To distinguish this case, which is also initially treated in this lecture, a further distinction is made:

- Weak undulator $K_\mathrm{u} \ll 1$:

  Undulator in the strict sense with quasi-monochromatic radiation.

- Strong undulator $K_\mathrm{u} \gtrsim 1$:

  Undulator with radiation of a spectrum with several harmonics.

The wiggler is then a limiting case of the strong undulator. The distinction between these three cases is not sharp. In practice, undulators are implemented as strong undulators, but their field amplitude can be varied up to the range of the weak undulator. We will see that in this way the energy of the emission lines of the undulator can be varied, i.e. the undulator can be tuned.

In addition to the types mentioned here and discussed in more detail below, other types of insertion devices are in use:

- Wavelength shifter

  A limiting case of a 3-pole wigglers with a very high field

- Helical undulator

  Undulator with two phase-shifted transverse field components
  $\rightarrow$ helical trajectory
  $\rightarrow$ emission of circularly polarised radiation

- Modulated undulators

  e.g. amplitude-modulated field or field amplitude linearly decreasing in z (*tapered undulator*) for certain desired properties of the emitted radiation.

6 The weak undulator

6.1 Qualitative approach

Before we look at the mathematical description of the properties of undulator radiation, let us first consider a qualitative understanding of how undulators work. It should be noted that the following 'reflection represents only one of several instructive qualitative approaches to undulator radiation. The interested listener and reader is referred to the beautiful presentation in Hofmann 2004 for other approaches.

The weak undulator in the co-moving inertial system

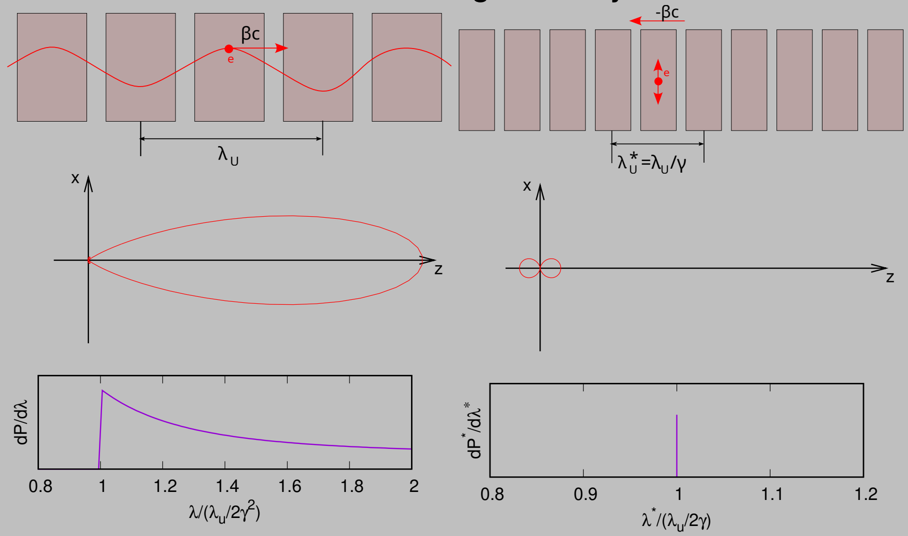

In this figure, the particle motion in the inertial system that is also moving with the particle is considered. The reduction of the mean drift velocity in the z direction is neglected, so that the particle motion results in a harmonic oscillation:

- Motion of the particle in the laboratory system with drift velocity βc
- Oscillation around $x = 0$ with frequency $\Omega_u = \frac{2\pi\beta c}{\lambda_u}$
- Motion of the undulator in the moving system with $-\beta c$
- Length contraction of the period in the co-moving system $\lambda_u^* = \lambda_u/\gamma$
- In the co-moving system: pure sinusoidal oscillation, radiation pattern of the Hertzian dipole, emission at a single frequency $\Omega_u^* = \Omega_u\gamma$
- Back-transformation into the laboratory system: forward-bundled radiation and Doppler-shifted frequency dependent on the observation angle $\omega_1 = \frac{\Omega_u^*}{\gamma(1-\beta\cos\vartheta)}$

6.2 Equation of motion and approximations

In order to be able to say more about the properties of the undulator radiation and the way in which these can be determined, we now take a closer look at the weak planar harmonic undulator. The procedure corresponds to that which we used to describe the spectral properties of normal synchrotron radiation: setting up the equation of motion, inserting it into the radiation field term and applying various approximations.

So, first the equation of motion of the particles for the general planar undulator is set up and then specialised by approximation for a weak undulator field.

The coordinate system

For the description, we choose the following coordinate system:

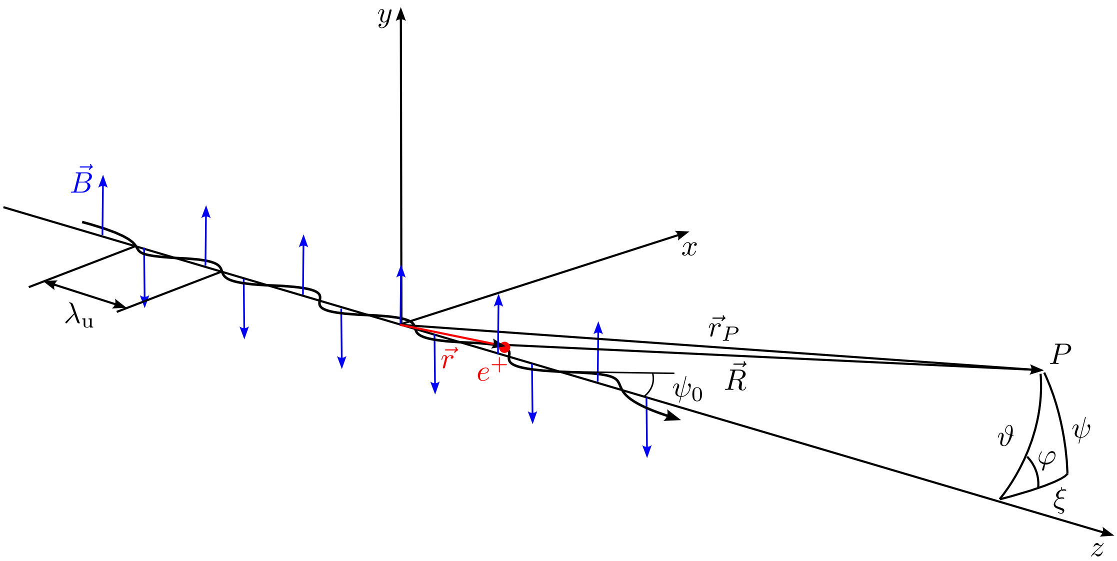

Figure 27: Representation of the coordinates important for describing the undulator radiation

The undulator field is assumed to be parallel to the y-axis in the centre plane and periodic with

$$\begin{aligned} &\text{period length:} && \lambda_u \\ &\text{number of periods:} && N_u \\ &\text{total length:} && L_u = N_u \lambda_u \end{aligned} \tag{6.1}$$

The undulator field in the centre plane $y = 0$ is given by

$$\vec{B}(x, 0, z) = B_0(0, \cos k_u z, 0) \tag{6.2}$$

Two remarks:

Remark (End fields). The undulator has a finite length $L_\mathrm{u} = N_\mathrm{u}\lambda_\mathrm{u}$, so its field is not strictly periodic. The influence of the end fields on the spectrum is neglected in our consideration. The end fields are also important for electron beam optics with respect to the transparency of the insertion device. Therefore, we will deal with the field termination of undulators and wigglers again later.

Remark (Field harmonics). In reality, an undulator field is usually not purely cosinusoidal but has higher harmonics. However, the following consideration is valid in principle for every Fourier component of the field and can therefore be easily generalised.

Equation of motion in the undulator

The magnitude of the particle velocity is constant

$$v = \beta c. \tag{6.3}$$

Initial conditions: The particle passes $z = 0$ at (emission) time $t' = 0$. In the chosen symmetrical field, then

$$z(0) = 0, \quad \dot{x}(0) = 0, \quad \dot{z}(0) = \beta c. \tag{6.4}$$

Thus, no transverse component of velocity at the origin.

The equations of motion now result from the Lorentz force

$$\vec{F} = m\gamma \begin{pmatrix} \ddot{x} \\ \ddot{y} \\ \ddot{z} \end{pmatrix} = e(\vec{v} \times \vec{B}) = eB_0 \begin{pmatrix} -\cos(k_\mathrm{u} z)\dot{z} \\ 0 \\ \cos(k_\mathrm{u} z)\dot{x} \end{pmatrix} \tag{6.5}$$

to

$$\ddot{x} = -\frac{eB_0}{m\gamma}\cos(k_\mathrm{u} z)\dot{z}, \qquad \ddot{z} = \frac{eB_0}{m\gamma}\cos(k_\mathrm{u} z)\dot{x}. \tag{6.6}$$

The equation for the x component can be integrated:

$$\dot{x} = -\frac{eB_0}{m\gamma k_\mathrm{u}}\sin(k_\mathrm{u} z). \tag{6.7}$$

For the z component, conservation of energy yields

$$\dot{x}^2 + \dot{z}^2 = \beta^2 c^2 \quad \Rightarrow \quad \dot{z} = \beta c\sqrt{1 - \frac{\dot{x}^2}{\beta^2 c^2}} \tag{6.8}$$

The properties of the radiation are determined from the radiation term of the retarded electric field:

$$\vec{E}(\vec{r}_P, t) = \frac{e}{4\pi\epsilon_0}\left[\frac{1}{c}\frac{\vec{n} \times [(\vec{n} - \vec{\beta}) \times \dot{\vec{\beta}}]}{(1 - \vec{\beta} \cdot \vec{n})^3 R}\right]_\mathrm{ret} \tag{6.9}$$

To calculate the radiation field from the trajectory, the following approximations are made:

- Approximation for the weak undulator: Neglect of the longitudinal oscillation component
- Far-field approximation: Observation from a large distance
- Ultrarelativistic approximation (analogous to normal synchrotron radiation)

Approximation for the weak undulator

Weak deflection means that the motion in the z direction can be approximated

$$\dot{z} = \beta c. \tag{6.10}$$

This equation can be integrated directly, yielding

$$x'(z) := \frac{\mathrm{d}x}{\mathrm{d}z} = \frac{\dot{x}}{\dot{z}} = -\frac{eB_0}{mc\beta\gamma k_\mathrm{u}} \sin k_\mathrm{u} z. \tag{6.11}$$

With the now exact definition of the undulator parameter

$$\boxed{K_\mathrm{u} := \beta\gamma\hat{x}' = \frac{eB_0}{mck_\mathrm{u}}} \tag{6.12}$$

we obtain for the trajectory in the weak undulator

$$\begin{aligned}
\vec{r}(t') &= \begin{pmatrix} \frac{K_\mathrm{u}}{\beta\gamma k_\mathrm{u}} \cos(\Omega_\mathrm{u} t') \\ 0 \\ \beta c t' \end{pmatrix} \\
\vec{\beta}(t') &= \begin{pmatrix} -\frac{K_\mathrm{u}}{\gamma} \sin(\Omega_\mathrm{u} t') \\ 0 \\ \beta \end{pmatrix} \\
\dot{\vec{\beta}}(t') &= \begin{pmatrix} \frac{K_\mathrm{u} c k_\mathrm{u} \beta}{\gamma} \cos(\Omega_\mathrm{u} t') \\ 0 \\ 0 \end{pmatrix}
\end{aligned} \tag{6.13}$$

with

$$\Omega_\mathrm{u} := k_\mathrm{u}\beta c. \tag{6.14}$$

This also allows the vector from the particle to the point of observation to be specified directly:

$$\begin{aligned}
\vec{R}(t') &= \vec{r}_\mathrm{p} - \vec{r}(t') \\
\vec{R}(t') &= r_\mathrm{p} \begin{pmatrix} \sin\vartheta\cos\varphi - \frac{K_\mathrm{u}}{r_\mathrm{p}\beta\gamma k_\mathrm{u}} \cos(\Omega_\mathrm{u} t') \\ \sin\vartheta\sin\varphi \\ \cos\vartheta - \frac{\beta c t'}{r_\mathrm{p}} \end{pmatrix}
\end{aligned} \tag{6.15}$$

Analogous to the treatment of normal synchrotron radiation, we carried out two further approximations. On the one hand, we again assume that the distance from the point of emission to the observer is large compared to the length of the path on which the particle is observed (i.e. here the length of the undulator), on the other hand we carry out the ultra-relativistic approximation:

Observation from a large distance

$$
\begin{aligned}
\text{Length of the undulator:} &\quad \frac{L_\mathrm{u}}{2r_\mathrm{p}} && \ll 1 \\
\text{Length of the observed trajectory:} &\quad \frac{L_\mathrm{u}}{2r_\mathrm{p}} \geq \frac{|\beta c t'|}{r_\mathrm{p}} && \ll 1, \\
\text{Oscillation amplitude:} &\quad \frac{K_\mathrm{u}}{r_\mathrm{p}\beta\gamma k_\mathrm{u}} && \ll 1
\end{aligned}
\tag{6.16}
$$

With this approximation, the absolute value of the distance vector $R(t')$ can be developed again up to the linear term. This results in

$$
R(t') = r_\mathrm{p} - \beta c t' \cos\vartheta - \frac{K_\mathrm{u}\sin\vartheta\cos\varphi}{\beta\gamma k_\mathrm{u}}\cos(\Omega_\mathrm{u} t'),
\tag{6.17}
$$

and thus for the relation between the reduced observer time t_p (defined analogously to normal synchrotron radiation) and emission time t'

$$
\begin{aligned}
t_\mathrm{p} := t - \frac{r_\mathrm{p}}{c} &= t' + \frac{R(t') - r_\mathrm{P}}{c} \\
&= t'(1 - \beta\cos\vartheta) - \frac{K_\mathrm{u}\sin\vartheta\cos\varphi}{\beta c\gamma k_\mathrm{u}}\cos(\Omega_\mathrm{u} t').
\end{aligned}
\tag{6.18}
$$

The second, oscillatory term turns out to be a phase modulation with a negligibly small amplitude and will be ignored in the following, so that a rather simple relation between reduced observer time and emission time results.

Overall, we obtain with this approximation for the terms to be used in the expression for the radiation field:

$$
\begin{aligned}
t_\mathrm{p} &= t'(1 - \beta\cos\vartheta) \\
1 - \vec{n}\cdot\vec{\beta} &= 1 - \beta\cos\vartheta \\
\vec{n}\times[(\vec{n}-\vec{\beta})\times\dot{\vec{\beta}}] &= \frac{c k_\mathrm{u} K_\mathrm{u}\cos(\Omega_\mathrm{u} t')}{2\gamma^3}
\begin{pmatrix} 1 - \beta\cos\vartheta - \sin^2\vartheta\cos^2\varphi \\ -\sin^2\vartheta\sin\varphi\cos\varphi \\ \sin\vartheta\cos\varphi(\beta - \cos\vartheta) \end{pmatrix}
\end{aligned}
\tag{6.19}
$$

Ultrarelativistic approximation

$$
\gamma \gg 1, \quad \vartheta \ll 1
\tag{6.20}
$$

ultimately leads to

$$
\begin{aligned}
1 - \vec{n}\cdot\vec{\beta} &= \frac{1 + \gamma^2\vartheta^2}{2\gamma^2} \\
\vec{n}\times\left((\vec{n}-\vec{\beta})\times\dot{\vec{\beta}}\right) &= \frac{c k_\mathrm{u} K_\mathrm{u}\cos\Omega_\mathrm{u} t'}{2\gamma^3}
\begin{pmatrix} 1 - \gamma^2\vartheta^2\cos 2\varphi \\ -\gamma^2\vartheta^2\sin 2\varphi \\ 0 \end{pmatrix}
\end{aligned}
\tag{6.21}
$$

as well as the relation between emission time and reduced observer time

$$t_\mathrm{p} = \frac{1+\gamma^2\vartheta^2}{2\gamma^2}t' \tag{6.22}$$

Accordingly, the frequency of motion Ω_u for the observer is "translated" into the frequency of the observed radiation

$$\omega_1 = \frac{2\gamma^2}{1+\gamma^2\vartheta^2}\Omega_\mathrm{u} =: \frac{\omega_{10}}{1+\gamma^2\vartheta^2} \tag{6.23}$$

with the fundamental frequency in the exact forward direction $\omega_{10} = 2\gamma^2\Omega_\mathrm{u}$.

Remark. Thanks to the simple relation of the time scales, the retarded fields in the case of undulator radiation can be represented relatively easily explicitly in both time and frequency space, in contrast to normal synchrotron radiation.

6.3 The radiation field

Inserting the approximating expressions into the radiation term of the retarded field and carrying out the Fourier transformation of this expression for a finite undulator with N_u periods leads to

$$\boxed{\begin{aligned} \vec{E}_\perp(t_\mathrm{p}) &= \begin{pmatrix} 1-\gamma^2\vartheta^2\cos 2\varphi \\ -\gamma^2\vartheta^2\sin 2\varphi \end{pmatrix} \frac{E_\mathrm{u}}{(1+\gamma^2\vartheta^2)^3}\cos\omega_1 t_\mathrm{p} \\ \vec{E}_\perp(\omega) &= \begin{pmatrix} 1-\gamma^2\vartheta^2\cos 2\varphi \\ -\gamma^2\vartheta^2\sin 2\varphi \end{pmatrix} \frac{E_\mathrm{u}}{(1+\gamma^2\vartheta^2)^3}\sqrt{\frac{\pi}{2}}\frac{N_\mathrm{u}}{\omega_1}\frac{\sin\left(\frac{\Delta\omega}{\omega_1}\pi N_\mathrm{u}\right)}{\frac{\Delta\omega}{\omega_1}\pi N_\mathrm{u}} \end{aligned}} \tag{6.24}$$

with

$$E_\mathrm{u} := \frac{e k_\mathrm{u} K_\mathrm{u}\gamma^3}{\pi\epsilon_0 r_\mathrm{p}} = \frac{4 r_0 c B_0 \gamma^3}{r_\mathrm{p}} \tag{6.25}$$

and

$$\Delta\omega := \omega - \omega_1$$

The "transition to an undulator of finite length" means that the electric field $\vec{E}_\perp(t_\mathrm{p})$ can only be observed within a time interval $[-N_\mathrm{u}\pi/\omega_1; N_\mathrm{u}\pi/\omega_1]$, and the above expression for the electric field in time must be multiplied by a box function over this interval.

For the transition to the frequency domain, this means that the Fourier integral is to be carried out only over this finite interval. This finite Fourier integral over the cosine term leads to the spectral function with a line width of $\Delta\omega/\omega_1 = 1/N_\mathrm{u}$. In the limit $N_\mathrm{u} \to \infty$, the spectral function tends towards a delta distribution.

Remark.

- E_x corresponds to the horizontal or σ-polarisation component with maximum amplitude E_u at $\vartheta = 0$
- E_y corresponds to the π polarisation component. This vanishes for $\vartheta = 0$ and in the horizontal ($\varphi = 0$) and vertical ($\varphi = \pi/2$) planes.

6.4 Properties of the radiation from the weak undulator

Radiated power and energy

The average power radiated by a particle in the undulator, i.e. the power averaged over one period, is given by

$$P_\mathrm{u} = \frac{r_0 c m c^2 \gamma^2 k_\mathrm{u}^2 K_\mathrm{u}^2}{3}, \tag{6.26}$$

and from this, the energy radiated when passing through the undulator

$$W_\mathrm{u} = \frac{P_\mathrm{u} L_\mathrm{u}}{c}. \tag{6.27}$$

The power radiated by a particle stream I thus becomes

$$P_{\mathrm{u}I} = \frac{I W_\mathrm{u}}{e} = \frac{r_0 m c^2 \gamma^2 I k_\mathrm{u}^2 K_\mathrm{u}^2 N_\mathrm{u} \lambda_\mathrm{u}}{3e} \tag{6.28}$$

Spectral-angular power distribution

$$\boxed{\frac{\mathrm{d}^2 P_\mathrm{u}}{\mathrm{d}\Omega \mathrm{d}\omega} = P_\mathrm{u} \gamma^2 (F_{\mathrm{u}\sigma}(\vartheta, \varphi) + F_{\mathrm{u}\pi}(\vartheta, \varphi)) f_N(\Delta\omega)} \tag{6.29}$$

with the angular distribution functions

$$F_{\mathrm{u}\sigma}(\vartheta, \varphi) = \frac{3}{\pi} \frac{(1 - \gamma^2 \vartheta^2 \cos 2\varphi)^2}{(1 + \gamma^2 \vartheta^2)^5}, F_{\mathrm{u}\pi}(\vartheta, \varphi) = \frac{3}{\pi} \frac{(\gamma^2 \vartheta^2 \sin 2\varphi)^2}{(1 + \gamma^2 \vartheta^2)^5} \tag{6.30}$$

and the spectral function

$$f_N(\Delta\omega) = \frac{N_\mathrm{u}}{\omega_1} \left(\frac{\sin(\pi N_\mathrm{u} \Delta\omega / \omega_1)}{\pi N_\mathrm{u} \Delta\omega / \omega_1} \right)^2 \tag{6.31}$$

with

$$\int_{-\infty}^{\infty} f_N(\Delta\omega) \mathrm{d}\omega = 1 \tag{6.32}$$

Spectral function of the undulator radiation

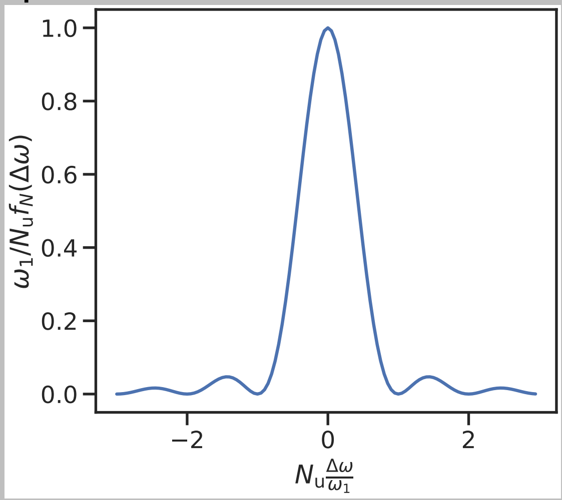

Spectral function of the undulator radiation for given undulator properties N_u, λ_u, $K_\mathrm{u} \ll 1$, electron energy γ and observation angle ϑ.
The relative width of the spectral function is $1/N_\mathrm{u}$.

Angular distribution

As we have just seen, the integration over all energies leads to the spectral function being integrated to 1. The angular distribution is then given by the two angular distribution functions.

Undulator radiation: angular power distribution

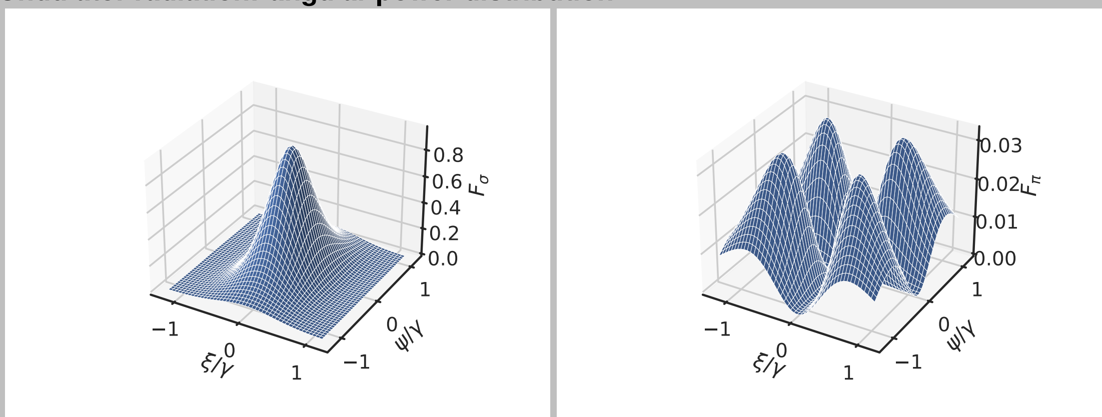

Figure 28: Power distribution of the energy-integrated undulator radiation for σ and π polarisation

The variance over the opening angle is obtained in the same way as for normal synchrotron radiation, i.e.

$$\vartheta_\mathrm{RMS} = \frac{1}{\gamma} \tag{6.33}$$

However, if one looks at the angular distribution specifically for the fundamental frequency ω_{10} and notes that

$$\omega_1 = \frac{\omega_{10}}{1+\gamma^2\vartheta^2} \tag{6.34}$$

there is a correlation between frequency and angular distribution, the variance over the opening angle is obtained as

$$\vartheta_{\mathrm{RMS}}(\omega_{10}) = \frac{\sqrt[4]{3\pi}}{\pi}\frac{1}{\gamma\sqrt{N_\mathrm{u}}} \tag{6.35}$$

Spectral radiation power distribution

The sinc-shaped spectral distribution results for a single electron whose radiation is detected at exactly one particular observation angle. In reality, there is always an electron ensemble with a *distribution of the directions of motion* and a detector with a finite aperture, i.e. *integration over a finite solid angle* is present. Therefore, a Doppler-broadened spectral distribution is always observed.

To illustrate this fact, let us consider the angle-integrated spectrum of the radiated power. To do this, the observation angle ϑ must essentially be converted into a frequency.

For simplicity, let us consider the case $N_\mathrm{u} \to \infty$. Then the spectral function goes into a delta distribution and the relationship between observed frequency and observation angle is one-to-one:

$$\begin{aligned}\omega_1 &= \frac{\omega_{10}}{1+\gamma^2\vartheta^2}\\ \mathrm{d}\omega_1 &= -2\omega_{10}\gamma^2\left(\frac{\omega_1}{\omega_{10}}\right)^2\vartheta\mathrm{d}\vartheta\end{aligned} \tag{6.36}$$

This means that

$$\frac{\mathrm{d}P}{\mathrm{d}\omega_1} = \frac{1}{2\omega_{10}\gamma^2}\left(\frac{\omega_{10}}{\omega_1}\right)^2\frac{\mathrm{d}P}{\vartheta\mathrm{d}\vartheta} = \frac{1}{2\omega_{10}\gamma^2}\left(\frac{\omega_{10}}{\omega_1}\right)^2\int_0^{2\pi}\frac{\mathrm{d}P}{\mathrm{d}\Omega}\mathrm{d}\varphi \tag{6.37}$$

Evaluation of the integral over the angular distribution functions leads to the spectral functions of the infinitely long undulator

$$\begin{aligned}\frac{\mathrm{d}P_{\mathrm{u}\sigma}}{\mathrm{d}\omega_1} &= \frac{3P_\mathrm{u}}{\omega_{10}}\frac{\omega_1}{\omega_{10}}\left(\frac{1}{2}-\frac{\omega_1}{\omega_{10}}+\frac{3}{2}\left(\frac{\omega_1}{\omega_{10}}\right)^2\right)\\ \frac{\mathrm{d}P_{\mathrm{u}\pi}}{\mathrm{d}\omega_1} &= \frac{3P_\mathrm{u}}{\omega_{10}}\frac{\omega_1}{\omega_{10}}\left(\frac{1}{2}-\frac{\omega_1}{\omega_{10}}+\frac{1}{2}\left(\frac{\omega_1}{\omega_{10}}\right)^2\right)\\ \frac{\mathrm{d}P_\mathrm{u}}{\mathrm{d}\omega_1} &= \frac{3P_\mathrm{u}}{\omega_{10}}\frac{\omega_1}{\omega_{10}}\left(1-2\frac{\omega_1}{\omega_{10}}+2\left(\frac{\omega_1}{\omega_{10}}\right)^2\right)\end{aligned} \tag{6.38}$$

Undulator radiation: angle-integrated spectral distribution

$$\frac{\mathrm{d}P_{\mathrm{u}\sigma}}{\mathrm{d}\omega_1} = \frac{3P_\mathrm{u}}{\omega_{10}}\frac{\omega_1}{\omega_{10}}\left(\frac{1}{2} - \frac{\omega_1}{\omega_{10}} + \frac{3}{2}\left(\frac{\omega_1}{\omega_{10}}\right)^2\right)$$

$$\frac{\mathrm{d}P_{\mathrm{u}\pi}}{\mathrm{d}\omega_1} = \frac{3P_\mathrm{u}}{\omega_{10}}\frac{\omega_1}{\omega_{10}}\left(\frac{1}{2} - \frac{\omega_1}{\omega_{10}} + \frac{1}{2}\left(\frac{\omega_1}{\omega_{10}}\right)^2\right)$$

$$\frac{\mathrm{d}P_\mathrm{u}}{\mathrm{d}\omega_1} = \frac{3P_\mathrm{u}}{\omega_{10}}\frac{\omega_1}{\omega_{10}}\left(1 - 2\frac{\omega_1}{\omega_{10}} + 2\left(\frac{\omega_1}{\omega_{10}}\right)^2\right)$$

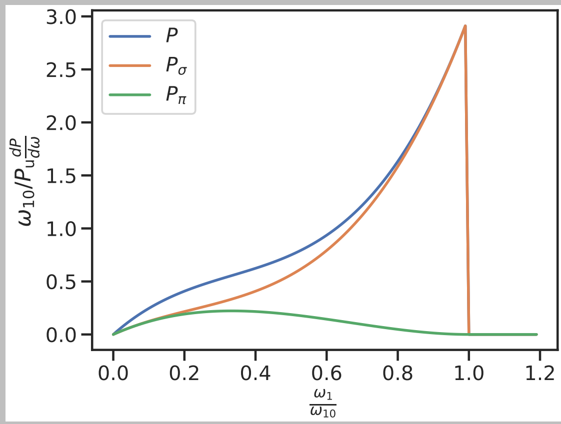

Remark. Finite number of periods: → convolution with spectral function

For undulators with a finite number of periods, this is to be convolved with the spectral function $f_N(\Delta\omega)$. This leads in particular to a softening of the sharp edge at ω_{10}.

The strong Doppler broadening effect visible in the spectrum also occurs in a similar way as a result of the finite emittance of the electron beam and the finite angular acceptance of the detector.

Photon flux

Finally, a note on photon flux.

As in the case of normal synchrotron radiation, the spectral power density of the radiation can be translated into a spectral photon flux by means of ad hoc quantisation. For an undulator of length L_u with a particle current I, this yields the mean total photon flux in an analogous way to normal synchrotron radiation

$$\dot{n}_{\mathrm{u}I} = \frac{2\pi\alpha_\mathrm{f} I K_\mathrm{u}^2 N_\mathrm{u}}{3e} \tag{6.39}$$

with the fine structure constant introduced for the sake of brevity

$$\alpha_f = \frac{e^2}{2\epsilon_0 c h}$$

Remark. Unlike normal synchrotron radiation, both the total radiation power and the photon energy scale with γ^2. This means that the total number of photons emitted is independent of γ!

The total photon flux is, however, relatively uninteresting for the experiment, since it usually uses the monochromatic photon flux in a small solid angle around the beam axis.

A good measure for this is the photon flux density on the beam axis and at the fundamental frequency ω_{10}:

$$\boxed{\left.\frac{\mathrm{d}^2\dot{n}_{\mathrm{u}I}}{\mathrm{d}\Omega\mathrm{d}\omega/\omega}\right|_{\omega_{10}} = \frac{\alpha_\mathrm{f}\gamma^2 I K_\mathrm{u}^2 N_\mathrm{u}^2}{e}} \tag{6.40}$$

This shows the intensity amplification of the undulator for the emission wavelength, i.e. under the condition of constructive interference: The photon flux for this wavelength scales with N_u^2, while the total photon flux scales with N_u.

The advantage of the undulator over the bending magnet or the wiggler lies not only in the high intensity at a certain wavelength, which, as we shall see in a moment, can be selected within certain limits, but also in the low photon flux at all other wavelengths, which is mainly reflected in heat load on the X-ray optical elements.

References

Hofmann, Albert (2004). *The Physics of Synchrotron Radiation*. Cambridge Monographs on Particle Physics, Nuclear Physics and Cosmology. Cambridge: Cambridge University Press. ISBN: 978-0-521-30826-7. DOI: 10.1017/CBO9780511534973.